

1-2015

Viscoelastic effects on electrokinetic particle focusing in a constricted microchannel

Xinyu Lu

John DuBose

Sang Woo Joo

Shizhi Qian
Old Dominion University

Xiangchun Xuan

Follow this and additional works at: https://digitalcommons.odu.edu/mae_fac_pubs

 Part of the [Biophysics Commons](#), and the [Nanoscience and Nanotechnology Commons](#)

Repository Citation

Lu, Xinyu; DuBose, John; Joo, Sang Woo; Qian, Shizhi; and Xuan, Xiangchun, "Viscoelastic effects on electrokinetic particle focusing in a constricted microchannel" (2015). *Mechanical & Aerospace Engineering Faculty Publications*. 2.
https://digitalcommons.odu.edu/mae_fac_pubs/2

Original Publication Citation

Lu, X. Y., DuBose, J., Joo, S. W., Qian, S. Z., & Xuan, X. C. (2015). Viscoelastic effects on electrokinetic particle focusing in a constricted microchannel. *Biomicrofluidics*, 9(1). doi: 10.1063/1.4906798

Viscoelastic effects on electrokinetic particle focusing in a constricted microchannel

Xinyu Lu,¹ John DuBose,¹ Sang Woo Joo,^{2,a)} Shizhi Qian,³ and Xiangchun Xuan^{1,a)}

¹*Department of Mechanical Engineering, Clemson University, Clemson, South Carolina 29634-0921, USA*

²*School of Mechanical Engineering, Yeungnam University, Gyongsan 712-719, South Korea*

³*Institute of Micro/Nanotechnology, Old University, Norfolk, Virginia 23529, USA*

(Received 18 December 2014; accepted 15 January 2015; published online 22 January 2015)

Focusing suspended particles in a fluid into a single file is often necessary prior to continuous-flow detection, analysis, and separation. Electrokinetic particle focusing has been demonstrated in constricted microchannels by the use of the constriction-induced dielectrophoresis. However, previous studies on this subject have been limited to Newtonian fluids only. We report in this paper an experimental investigation of the viscoelastic effects on electrokinetic particle focusing in non-Newtonian polyethylene oxide solutions through a constricted microchannel. The width of the focused particle stream is found NOT to decrease with the increase in DC electric field, which is different from that in Newtonian fluids. Moreover, particle aggregations are observed at relatively high electric fields to first form inside the constriction. They can then either move forward and exit the constriction in an explosive mode or roll back to the constriction entrance for further accumulations. These unexpected phenomena are distinct from the findings in our earlier paper [Lu *et al.*, *Biomicrofluidics* **8**, 021802 (2014)], where particles are observed to oscillate inside the constriction and not to pass through until a chain of sufficient length is formed. They are speculated to be a consequence of the fluid viscoelasticity effects. © 2015 AIP Publishing LLC. [<http://dx.doi.org/10.1063/1.4906798>]

I. INTRODUCTION

Focusing suspended particles in a fluid into a single file is often important and necessary in order to continuously detect, analyze, and sort them for numerous applications.^{1,2} Sheath flow focusing is the most routine particle focusing method in microfluidic devices because it uses sheath fluids to pinch the particulate solution and works effectively for particles of essentially any size.^{3,4} However, a precise control of the flow rate and a large consumption of the sheath fluid are the drawbacks of this method. In contrast, sheathless focusing of particles relies on a force field to act directly on the suspended particles and move them laterally for alignment, which is often flexible in control and simple in operation. So far, a variety of forces have been demonstrated to focus particles in microfluidic devices, which can be either externally imposed like acoustic,⁵ electric,⁶ magnetic,⁷ optical⁸ forces, etc., or internally induced like inertial,⁹ viscoelastic,^{10–13} hydrodynamic,¹⁴ and dielectrophoretic¹⁵ forces. However, these methods often suffer from low effectiveness when working with small particles due to the strong size-dependence of nearly, if not all, every force field.^{1,2}

Electrokinetic flow is an efficient means to transport fluids and particles in microfluidic devices under DC electric fields due to its excellent scalability and easy connection.^{16,17} It has been exploited to drive both the particulate and sheath solutions in sheath flow focusing of particles.^{18,19} It has also been demonstrated to pump the particulate solution while simultaneously

^{a)}Authors to whom correspondence should be addressed. Electronic addresses: swjoo@yu.ac.kr and xcxuan@clemson.edu

manipulating the suspended particles into equilibrium position(s) for a sheathless focusing. The latter function is achieved primarily through the use of a geometry-induced dielectrophoretic motion, which is the translation of particles (either charged or neutral) in response to electric field gradients.¹⁹ Such an insulator-based dielectrophoretic focusing of particles has been demonstrated in both constricted^{20,21} and curved^{22,23} microchannels. However, all these studies have been limited to Newtonian fluids only, in which fluid electroosmosis and particle electrophoresis are simply a linear function of the applied DC electric field. As many of the fluids used in capillary electrophoresis and microfluidic devices, such as polymer solutions and bodily fluids, are complex,^{24–32} it is important from the aspects of both fundamentals and applications to study how electrokinetic particle focusing may be affected by the fluid non-Newtonian effects.

While a number of theoretical studies have been reported on, for example, the shear thinning/thickening and viscoelastic effects on fluid electroosmosis and particle electrophoresis in non-Newtonian fluids,^{33–45} much less has been done through experimental investigation and validation. In a recent study from Chang and Tsao,⁴⁶ a significant drag reduction was observed in electroosmotic flow of polymer solutions. This was attributed to the polymer depletion in the electric double layer, and the drag reduction was found to increase with the ratio of the polymer size to the electric double layer thickness. In a more recent study, Bryce and Freeman⁴⁷ observed an extensional instability in the electroosmotic flow of dilute polymer solutions through a microchannel constriction, which, however, was found later by the same group to actually reduce the fluid mixing as compared to that in polymer-free fluids.⁴⁸

Very recently, we have conducted an experimental study of electrokinetic particle motion in polyethylene oxide (PEO) solutions through a microchannel constriction.⁴⁹ No apparent electrokinetic focusing of particles was observed, which is distinctly different from what has been previously demonstrated in Newtonian fluids.^{20,21} Instead, an unexpected particle oscillation occurred in the constriction, which continued until a particle chain of sufficient length was formed. This phenomenon is found to persist for particles of different sizes as long as they move along with the electric field. It also holds true when the applied DC electric field or the PEO concentration is varied. However, as we will present in this experimental work, particles that move against the electric field in PEO solutions do not experience such oscillations in a constricted microchannel. They can be electrokinetically focused with a different trend from that in Newtonian fluids when the electric field is increased. Moreover, particle aggregations can be formed inside the constriction with subsequent interesting behaviors.

II. EXPERIMENT

A. Preparation of non-Newtonian fluids and particle suspensions

Non-Newtonian fluids were prepared by dissolving PEO powder (Sigma-Aldrich USA, average molecular weight $M_w = 4 \times 10^6$ Da) into 1 mM phosphate buffer at concentrations of 50 ppm (i.e., dissolving 50 mg PEO powder into 1 l buffer), 100 ppm, 200 ppm, and 500 ppm, respectively. It is important to note that PEO solutions at similar concentrations have been frequently used in the literature to study the viscoelasticity effects on hydrodynamic fluid flows^{50–52} and particle motions^{53–55} in microchannels. The concentration we used are all lower than the overlapping concentration ($c^* = 547$ ppm⁴⁹) of the PEO, indicating that all four prepared solutions are in the dilute regime. The shear viscosities of these solutions were measured in a Couette geometry (ARES LS/M, TA instruments) at room temperature. Nearly constant values of 1.1 mPa s, 1.2 mPa s, 1.4 mPa s, and 2.0 mPa s, respectively, were obtained for the four PEO concentrations in the range of shear rate from 50 s^{-1} to 1000 s^{-1} . The relaxation times of these solutions were estimated to be 4.07 ms, 6.39 ms, 10.01 ms, and 18.17 ms, respectively. The detailed process for calculating these values and the list of other properties of the PEO solutions can be referred to Lu *et al.*⁴⁵

The non-Newtonian particle suspensions were made by re-suspending polystyrene spheres of $3.1 \mu\text{m}$, $4.8 \mu\text{m}$, and $9.9 \mu\text{m}$ in diameter (Thermo Scientific) in the PEO solution(s) to a final concentration of about 10^6 particles per milliliter. To illustrate the viscoelastic effects, $9.9 \mu\text{m}$

particles were also re-suspended in the base fluid of the PEO solutions, i.e., 1 mM pure buffer, which is a Newtonian fluid, for a direct comparison. A small amount of Tween 20 (0.5% in volume ratio, Fisher Scientific) was added to both the Newtonian and non-Newtonian particle suspensions for the purpose of suppressing particle-wall and particle-particle adhesions. The effective electric conductivity, σ_p , of particles was calculated from $\sigma_p = 4\sigma_s/d$ with $\sigma_s = 1$ nS being the particle's surface conductance and d the particle diameter.⁵⁶ It was found to be 12.90, 8.33, and 4.04 $\mu\text{S}/\text{cm}$ for 3.1, 4.8 and 9.9 μm -diameter particles, respectively. Because these conductivity values are all much smaller than that of the suspending fluid (approximately 200 $\mu\text{S}/\text{cm}$), negative dielectrophoresis (DEP) are expected to occur under the application of DC electric fields in both the Newtonian and non-Newtonian fluids.

B. Experimental setup

The standard soft lithography method is used in the fabrication of microchannels, as detailed by Lu *et al.*⁴⁹ The polydimethylsiloxane (PDMS) microchannel is sealed from bottom by a regular glass slide, through which Joule heating can be dissipated relatively easily to avoid significant temperature rises in the particle suspensions.⁵⁷ The 40 μm -deep microchannel is overall 1 cm long and 400 μm wide with a constriction of 200 μm length and 40 μm width in the middle. The electrokinetic fluid and particle motions in the microchannel were driven by DC electric fields, supplied by a DC power supply (Glassman High Voltage Inc., High Bridge) through the end-channel reservoirs. The electric field magnitude was kept no more than 500 V/cm in order to minimize Joule heating effects in the constriction region.⁵⁸ Pressure-driven fluid and particle motions were eliminated by balancing the liquid heights in the inlet and outlet reservoirs prior to each test. Particle transport in the microchannel constriction was visualized and recorded through an inverted microscope (Nikon Eclipse TE2000U, Nikon Instruments) with a CCD camera (Nikon DS-Qi1Mc) at a rate of 15 frames per second. The videos and images obtained were post-processed using the Nikon imaging software (NIS-Elements AR 2.3). Particle streak images were obtained by superimposing a sequence of 600 images.

C. Measurement of electrokinetic particle mobility

The electrokinetic velocity of particles, \mathbf{U}_{EK} , in a microchannel is the vector addition of electroosmotic fluid velocity, \mathbf{U}_{EO} , and electrophoretic particle velocity, \mathbf{U}_{EP} ,

$$\mathbf{U}_{EK} = \mathbf{U}_{EO} + \mathbf{U}_{EP} = \frac{\varepsilon(\zeta_p - \zeta_w)}{\eta} \mathbf{E}, \quad (1)$$

where ε is the dielectric permittivity of the suspending fluid, ζ_p is the zeta potential of the particle, ζ_w is the zeta potential of the channel wall due to the spontaneous formation of electric double layer at the fluid-wall interface, η is the fluid dynamic viscosity, and \mathbf{E} is the applied DC electric field. It was determined from the measured particle travelling distance over a time interval in the microchannel. The measuring region is distant from the channel entrance and the constriction, so that the local electric field and particle velocity both remain constant. The electrokinetic mobility of particles, μ_{EK} , was calculated from the electrokinetic velocity divided by the local DC electric field (numerically computed in COMSOL, Burlington, MA),

$$\mu_{EK} = \frac{\varepsilon(\zeta_p - \zeta_w)}{\eta}, \quad (2)$$

which is apparently a function of the physicochemical properties of the tested fluid-particle-channel system. In our experiments, particles travel from the cathode to the anode in both the Newtonian and non-Newtonian solutions, i.e., $\mu_{EK} < 0$, which indicates the dominance of particle electrophoresis over fluid electroosmosis. This is because the electroosmotic fluid motion is nearly always from the anode to the cathode, i.e., $\zeta_w < 0$ ^{16,17,30} and hence $\zeta_p < \zeta_w < 0$ or $|\zeta_p| > |\zeta_w|$.

The observed direction of the electrokinetic motion of particles from Thermo Scientific in the current work is contrary to that of the particles from Sigma Aldrich used in our previous paper.⁴⁹ Therefore, fluid electroosmosis should dominate over particle electrophoresis in the latter case, leading to $\zeta_w < \zeta_p < 0$ or $|\zeta_w| > |\zeta_p|$ based on a similar analysis to the above. While both types of particles are made of polystyrene as per the product manuals, only the particles from Thermo Scientific are fluorescently dyed. This may be responsible for the observed difference in particle zeta potential, ζ_p , between the two types of particles. The electrokinetic particle mobility is found to be nearly independent of the particle size in all the solutions tested in this work. However, the addition of PEO into the buffer solution increases the particle mobility, which is also different from those particles used in our previous paper.⁴⁹ Specifically, the measured particle mobility is $2.6 \times 10^{-8} \text{ m}^2/(\text{V}\cdot\text{s})$ in the 500 ppm PEO solution, and found to decrease by less than 10% when the PEO concentration is varied from 500 ppm to 50 ppm. In contrast, the electrokinetic particle mobility is only $1.3 \times 10^{-8} \text{ m}^2/(\text{V}\cdot\text{s})$ in the Newtonian buffer solution. Since the viscosity of the 500 ppm PEO solution is nearly twice that of the Newtonian buffer, the wall zeta potential, ζ_w , in the former is anticipated to be significantly smaller from Eq. (2). This can be attributed to the suppression of electroosmotic flows as a result of the coating of neutral PEO polymers onto the channel walls.⁵⁹ It is important to note that electrophoresis may also be suppressed by the PEO coating on particle surfaces, which requires a detailed study of the PEO effects on wall and particle zeta potentials.

III. RESULTS AND DISCUSSION

A. Comparison of electrokinetic particle focusing in Newtonian and non-Newtonian fluids

Fig. 1 compares in the form of superimposed images the electrokinetic focusing of $9.9 \mu\text{m}$ -diameter particles in Newtonian [(a)—1 mM buffer] and non-Newtonian [(b)—200 ppm PEO in 1 mM buffer] fluids through the microchannel constriction. The applied DC electric field increases from 100 V/cm to 400 V/cm for the images from left to right. At 100 V/cm particles exit the constriction in a narrower stream in both fluids. This focusing effect is attributed to the constriction-induced DEP that has been demonstrated in previous studies with Newtonian fluids.⁶⁰ As the electric field increases from 100 V/cm to 300 V/cm, the particle stream width in the pure buffer becomes thinner after the constriction (see Fig. 1(a)), indicating an enhanced electrokinetic focusing. This observation is consistent with previous studies^{20,21,60} and occurs due to the greater increase in dielectrophoretic motion than in electrokinetic motion at larger electric fields. Such a decrease in the focused particle stream width also agrees reasonably with the predictions of a Lagrangian tracking method-based numerical model in COMSOL (data not shown). In the PEO solution, however, the electrokinetic particle focusing turns out NOT to increase with the applied electric field. As measured directly from the top edge of the images (i.e., where particles travel out of the images) in Fig. 1(b), the focused particle stream width (note the wider particle stream, the worse focusing) actually increases from $176 \mu\text{m}$ to $216 \mu\text{m}$ and $240 \mu\text{m}$ when the electric field is increased from 100 V/cm to 300 V/cm. Moreover, the particles at the edges of the focused streams are scattered, which seems not to be a strong function of the applied electric field. This dispersion phenomenon is not obvious for particles in the Newtonian buffer (see Fig. 1(a)).

To further verify the trend of this reduced particle focusing with electric field, we also studied the electrokinetic motion of similar sized particles from other companies in the same PEO solution: one is the $9.9 \mu\text{m}$ -diameter particle from Duke Scientific, and the other is the $10.14 \mu\text{m}$ -diameter particle from Bangs Laboratories. Each type of these particles moved from the cathode to the anode though at a dissimilar electrokinetic mobility from the particles in Fig. 1(b). We observed a similar trend of weakened electrokinetic particle focusing with an increase in electric field for both particles (data not shown). Thus, the viscoelasticity of the PEO solution is believed to be a factor contributing to this phenomenon. We speculate that fluid viscoelasticity draws disturbances to electrokinetic particle motion in the constriction region due to the shear-induced electroosmotic fluid instability that has been recently demonstrated

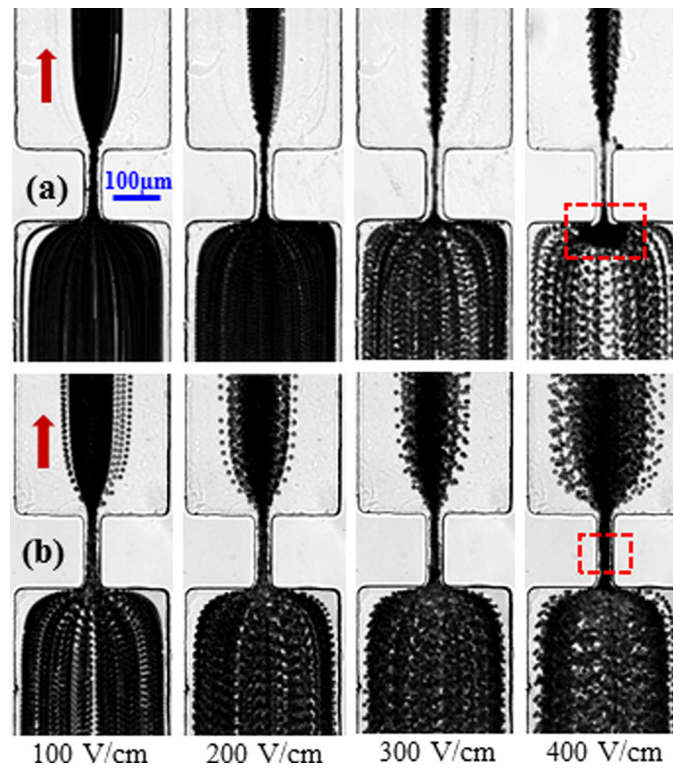


FIG. 1. Superimposed images illustrating the effects of fluid viscoelasticity on electrokinetic focusing of $9.9\ \mu\text{m}$ particles in a constricted microchannel under various DC electric fields: (a) Newtonian fluid (1 mM buffer); (b) non-Newtonian fluid (200 ppm PEO in 1 mM buffer). The block arrows indicate the particle moving direction, which is from bottom to top in all images and against the electric field direction. The two dashed boxes on the right-most images highlight the regions in which the particle trapping is initiated. A clear demonstration of the observed particle trapping phenomenon in the PEO solution is presented as snapshot images in Fig. 2. Note that the widths of the focused particle streams referred to in the text (see also Figs. 3 and 4) were all measured directly from the top edge of the images where particles travel out.

experimentally^{47,48} and numerically.⁶¹ Such a de-focusing effect increases more quickly with electric field than the constriction-induced dielectrophoretic force does, and consequently, the electrokinetic particle focusing gets worse at higher electric fields. In addition, it is important to note that the reported particle oscillations and formation of particle chains in our previous paper⁴⁹ are absent from the constriction in this work for all the three types of particles under test. This change appears to be associated with the direction of the electrokinetic particle motion, which may be due to the dominant particle electrophoresis over fluid electroosmosis in this work as analyzed earlier.

When the DC electric field applied was further increased to 400 V/cm, particles in the Newtonian fluid started being trapped at the constriction entrance (highlighted by a dashed box on the right-most image in Fig. 1(a)). This happens because the constriction-induced DEP becomes strong enough to counterbalance the electrokinetic motion in the streamline direction. However, particles cannot be fully trapped until an even higher electric field is applied because of the influence of the trapped particles on the local electric field gradients.⁶² In contrast, electrokinetic particle trapping also occurs in the 200 ppm PEO solution at 400 V/cm but initiates inside the constriction (see the dashed-box highlighted region on the right-most image in Fig. 1(b)), and proceed in either a forward or a backward direction. As viewed from the first two images in Fig. 2(a) (Multimedia view), an aggregation of particles can be formed first inside the constriction, which was not observed in our previous work for particles moving in the electric-field direction.⁴⁹ More interestingly, the particle cluster can then either move forward, albeit slower than single particles, and exit the constriction in an explosive mode, as illustrated by the sequential images (see the thin arrows for the moving direction of the particle cluster) in

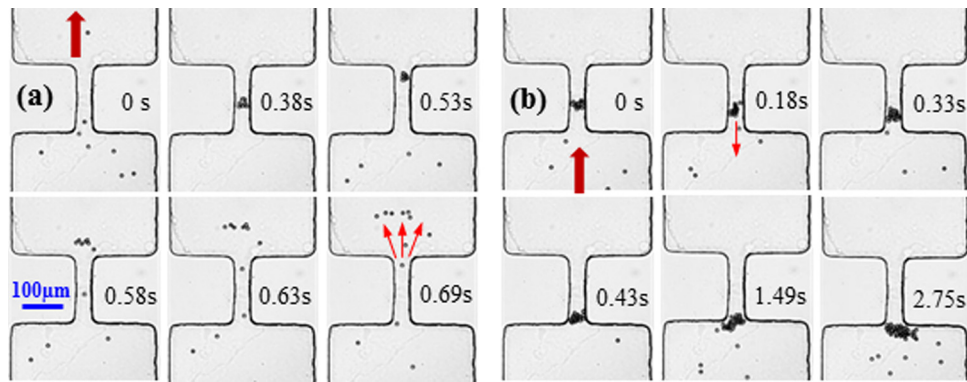


FIG. 2. Sequential images (with the relative time instants labeled) illustrating the forward ejection (a) and backward rolling (b) of $9.9\ \mu\text{m}$ -diameter particle aggregations in a non-Newtonian (200 ppm PEO) fluid through the microchannel constriction. The applied DC electric field is $400\ \text{V/cm}$. The block arrow indicates the overall particle moving direction in the microchannel, which is from bottom to top in all images and against the electric field direction (from top to bottom). The thin arrows indicate the moving directions of the particle clusters that are formed first inside the constriction. (Multimedia view) [URL: <http://dx.doi.org/10.1063/1.4906798.1>]

Fig. 2(a). Or alternatively, the particle cluster can roll back to the constriction entrance, where it grows continuously bigger and bigger with additional particles trapped. This process is demonstrated by the image sequence in Fig. 2(b) (Multimedia view), where, as seen from the labeled time instants, the backward-moving speed of the particle cluster within the constriction is comparable to the forward-moving speed of the particle cluster in Fig. 2(a). The formation and subsequent movement of particle aggregations in the constriction are speculated to be a consequence of the combined effects of viscoelastic instability^{47,48} and particle-particle interactions.⁶³ The exact mechanisms behind the observed phenomena in Figs. 1 and 2 are, however, currently unclear to us, for which a systematic study (especially theoretical) of the electroosmotic flow field and the fluid-particle-electric field interactions will be needed.

B. PEO concentration effect

Fig. 3 shows the effects of PEO concentration on the stream width of electrokinetically focused $9.9\ \mu\text{m}$ particles in the microchannel constriction. The applied DC electric field is varied from $100\ \text{V/cm}$ to $400\ \text{V/cm}$. The superimposed particle images in all tested PEO solutions (except for 200 ppm which is shown in Fig. 1) are presented in Fig. 4. The focused particle stream widths in all tested PEO solutions (including 50, 100, 200, and 500 ppm) are larger than that in the Newtonian fluid. This is mainly because the electrokinetic particle mobility in the latter is only approximately half of that in a PEO solution. Moreover, the constriction-induced particle DEP is smaller in a PEO solution due to its greater viscosity than the Newtonian buffer. Interestingly, particles in 50 ppm PEO solution behave similar to those in the Newtonian fluid (see Fig. 1(a)), and achieve an enhanced electrokinetic focusing (i.e., a decreased particle stream width) at a greater electric field. This indicates a relatively weak viscoelastic effect at a PEO concentration of 50 ppm, which is consistent with the observation in our previous study.⁴⁹ In contrast, the focused particle stream widths in all other tested PEO solutions expand with the increase of electric field. Moreover, a higher PEO concentration yields a weaker electrokinetic particle focusing. These phenomena are all supposed to result from the stronger viscoelastic effects when the PEO concentration is increased. Interestingly, the opposite trends of particle focusing vs. electric field in 50 and 100 ppm PEO solutions imply that there exists a critical PEO concentration at which particle focusing is insensitive to electric field. This may occur due to the balance of viscoelastic disturbances and dielectrophoretic focusing at the constriction, which will be studied in more details in the future. In addition, it is found that particle aggregations are not formed inside the constriction in 50 ppm PEO solution even at very high electric

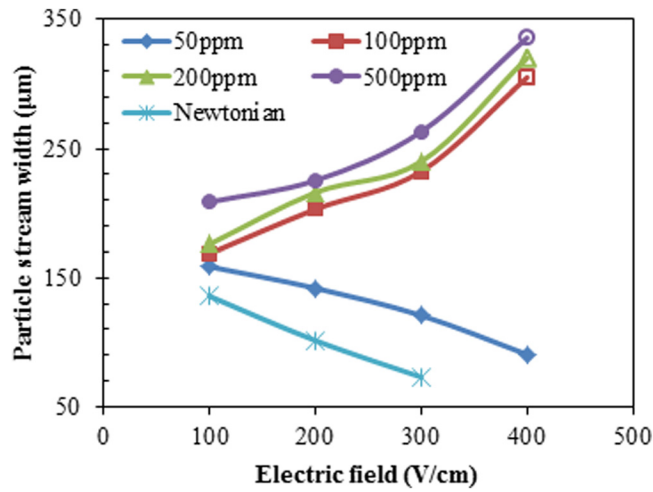


FIG. 3. Effects of PEO concentration (0, 50, 100, 200, and 500 ppm) on the stream width of electrokinetically focused $9.9 \mu\text{m}$ particles in the microchannel constriction at different DC electric fields. Error bars are included for only the data in the 500 ppm PEO solution for a better view, which are determined from the reading error in identifying the edges of the focused particle stream. The unfilled symbols represent the points at which particle aggregation was observed inside the constriction. The particle stream widths of these points are each measured from the superimposed images prior to the occurrence of particle aggregation.

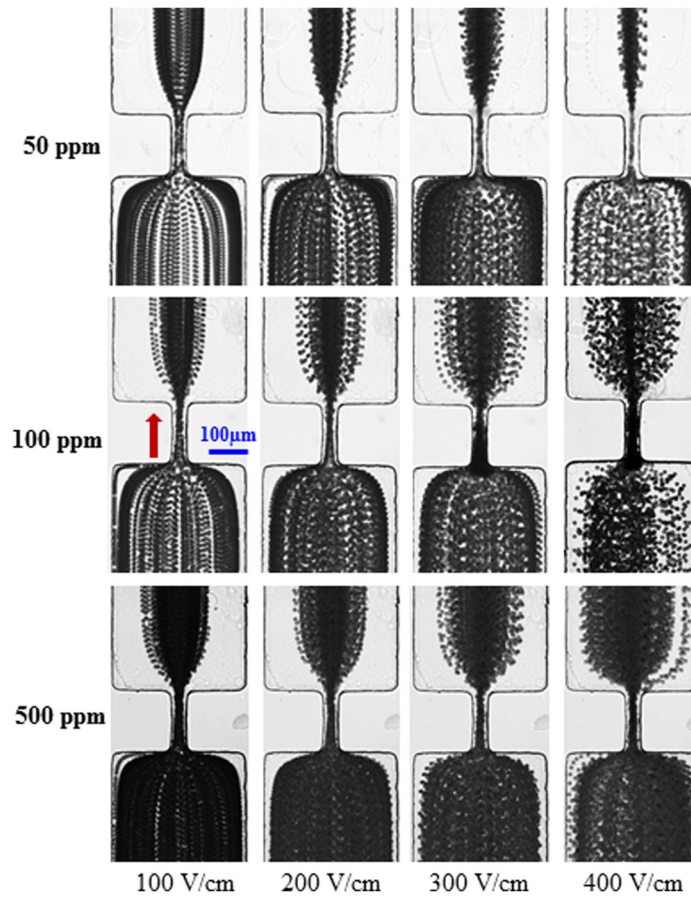


FIG. 4. Superimposed images illustrating the electrokinetic focusing of $10 \mu\text{m}$ -diameter particles in PEO solutions of various concentrations (0 and 200 ppm are referred to Fig. 1) under four different DC electric fields. The block arrow indicates the particle moving direction in all images.

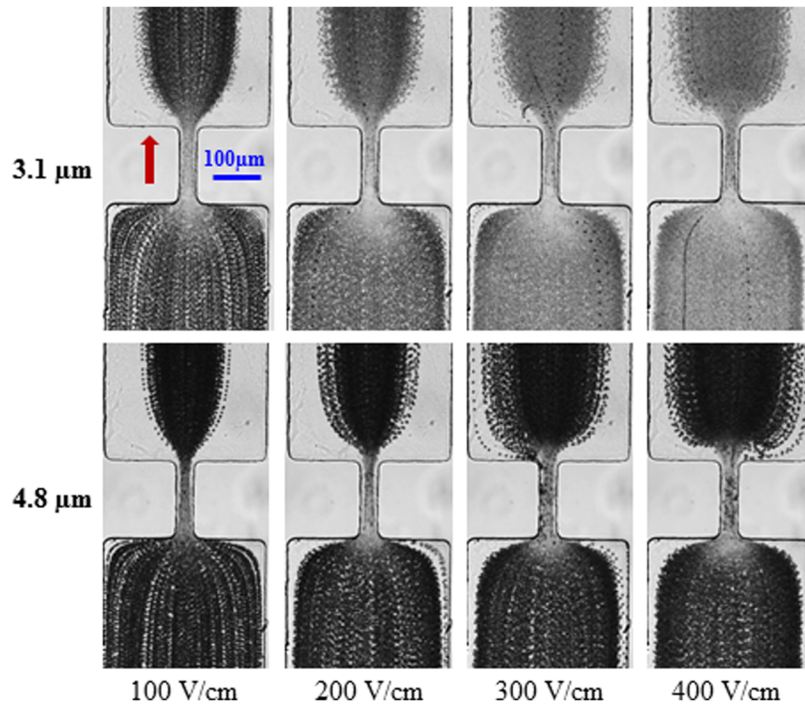


FIG. 5. Superimposed images illustrating the electrokinetic focusing of $3.1\ \mu\text{m}$ and $4.8\ \mu\text{m}$ -diameter particles (the images for $9.9\ \mu\text{m}$ particles are referred to Fig. 1) in 200 ppm PEO solution under four different DC electric fields. The block arrow indicates the particle moving direction in all images.

fields. However, they can easily occur at 400 V/cm (indicated by unfilled symbols in Fig. 3) in all other tested PEO solutions with similar behaviors to those illustrated in Fig. 2.

C. Particle size effect

To examine whether particle size contributes to the peculiar electrokinetic focusing phenomena in non-Newtonian fluids explained above, we also studied the electrokinetic motions of $3.1\ \mu\text{m}$ and $4.8\ \mu\text{m}$ particles in 200 ppm PEO solution in the constricted microchannel under

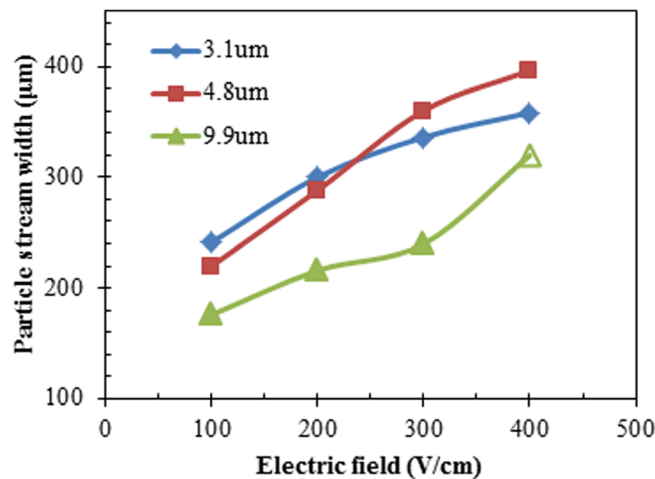


FIG. 6. Experimentally measured stream widths of the electrokinetically focused particles with different sizes in 200 ppm PEO solution in the constricted microchannel. The unfilled symbol for $9.9\ \mu\text{m}$ particles represents the point at which particle aggregation inside the constriction was observed. The particle stream width of this point is obtained from the superimposed images prior to the occurrence of particle aggregation.

various DC electric fields. The superimposed particle images are presented in Fig. 5. The experimentally measured stream widths of these particles at different electric fields are presented in Fig. 6 along with the ones for $9.9\ \mu\text{m}$ particles (see also Fig. 1(b)). The general trend that the electrokinetic focusing deteriorates with the increase of electric field persists for the two smaller particles. The extent of variation in the focused particle stream width with electric field, however, turns out to be dependent on particle size. At low electric fields (e.g., $100\ \text{V/cm}$), larger particles achieve, as expected, a better focusing than smaller ones because the former experience a stronger DEP while viscoelastic effects are still relatively weak. At high electric fields (e.g., $300\ \text{V/cm}$), the relationship among the three focused particle stream widths becomes complicated, as seen from Fig. 6. This is likely because viscoelastic effects are a complex function of both electric field and particle size, which requires further studies. In addition, similar forward and backward motions of particle clusters (see Fig. 2) are also observed within the constriction for both $3.1\ \mu\text{m}$ and $4.8\ \mu\text{m}$ particles but under an increased electric field of around $500\ \text{V/cm}$.

IV. CONCLUSIONS

We have experimentally studied the electrokinetic particle focusing in viscoelastic PEO solutions through a 10:1 ratio microchannel constriction. Particles are found to be less focused with the increase of the applied DC electric field, which is different from the focusing trend in Newtonian fluids. Also, particle aggregations are formed first inside the constriction at high electric fields while the purely dielectrophoretic trapping of particles in Newtonian fluids only occurs at the entrance of the constriction. More surprisingly, the particle aggregation can either move forward and be ejected from the constriction in an explosive manner, or roll back and grow bigger in size at the constriction entrance with more particles getting trapped. All these interesting phenomena are owed to the fluid viscoelasticity effects that are speculated to be a stronger function of electric field than DEP. The exact mechanisms underlying these phenomena deserve intensive future studies. We have also examined the effects of PEO concentration and particle size on the electrokinetic particle focusing behavior in the constricted microchannel. The viscoelastic perturbations to particle focusing and trapping are found to increase with the PEO concentration for larger particles. Since the observed particle focusing in all tested PEO solutions is worse than in the Newtonian fluid, we conclude that constriction-induced DEP is not a good option for electrokinetic focusing of particles suspended in non-Newtonian fluids. However, the demonstrated particle oscillation⁴⁹ and aggregation under relative low electric fields may find applications in bead-based assays.^{64,65}

ACKNOWLEDGMENTS

This work was partially supported by Clemson University through a departmental SGER (Small Grants for Exploratory Research) grant to X. Xuan.

- ¹D. A. Ateya, J. S. Erickson, P. B. Howell, Jr., L. R. Hilliard, J. P. Golden, and F. S. Ligler, *Anal. Bioanal. Chem.* **391**, 1485–1498 (2008).
- ²X. Xuan, J. Zhu, and C. Church, *Microfluid. Nanofluid.* **9**, 1–16 (2010).
- ³C. C. Chang, Z. Y. Huang, and R. J. Yang, *J. Micromech. Microeng.* **17**, 1479–1486 (2007).
- ⁴C. G. Tsai, H. H. Hou, and L. M. Fu, *Microfluid. Nanofluid.* **5**, 827–836 (2008).
- ⁵J. Shi, X. Mao, D. Ahmed, A. Colletti, and T. J. Huang, *Lab Chip* **8**, 221–223 (2008).
- ⁶I. F. Cheng, H. C. Chang, D. Hou, and H. C. Chang, *Biomicrofluidics* **1**, 021503 (2007).
- ⁷L. Liang, J. Zhu, and X. Xuan, *Biomicrofluidics* **5**, 034110 (2011).
- ⁸Y. Zhao, B. S. Fujimoto, G. D. M. Jeffries, P. G. Schiro, and D. T. Chiu, *Opt. Express* **15**, 6167–6176 (2007).
- ⁹H. Ramachandriah, S. Ardabili, A. M. Faridi, J. Gantelius, J. M. Kowalewski, G. Martensson, and A. Russom, *Biomicrofluidics* **8**, 034117 (2014).
- ¹⁰A. M. Leshansky, A. Bransky, N. Korin, and U. Dinnar, *Phys. Rev. Lett.* **98**, 234501 (2007).
- ¹¹S. Yang, J. Y. Kim, S. J. Lee, S. S. Lee, and J. M. Kim, *Lab Chip* **11**, 266–273 (2011).
- ¹²K. Kang, S. S. Lee, K. Hyun, S. J. Lee, and J. M. Kim, *Nat. Commun.* **4**, 2567 (2013).
- ¹³E. J. Lim, T. Ober, J. F. Edd, S. P. Desai, D. Neal, K. W. Bong, P. S. Doyle, G. H. McKinley, and M. Toner, *Nat. Commun.* **5**, 4120 (2014).
- ¹⁴S. Yan, J. Zhang, H. Chen, G. Alici, H. Du, Y. Zhu, and W. Li, *Biomicrofluidics* **8**, 064115 (2014).
- ¹⁵C. P. Jen and W. F. Chen, *Biomicrofluidics* **5**, 044105 (2011).

- ¹⁶D. Li, *Electrokinetics in Microfluidics* (Academic Press, 2004).
- ¹⁷H. C. Chang and L. Y. Yeo, *Electrokinetically-Driven Microfluidics and Nanofluidics* (Cambridge University Press, 2009).
- ¹⁸L. M. Fu, R. J. Yang, and G. B. Lee, *Anal. Chem.* **75**, 1905–1910 (2003).
- ¹⁹H. A. Pohl, *Dielectrophoresis: The Behavior of Neutral Matter in Non-Uniform Electric Fields* (Cambridge University Press, Cambridge, 1978).
- ²⁰C. Church, J. Zhu, G. Huang, T. R. Tzeng, and X. Xuan, *Biomicrofluidics* **4**, 44101 (2010).
- ²¹X. Xuan, S. Raghizadeh, and D. Li, *J. Colloid Interface Sci.* **296**, 743–748 (2006).
- ²²C. Church, J. Zhu, G. Huang, T. R. Tzeng, and X. Xuan, *Biomicrofluidics* **3**, 044109 (2009).
- ²³M. Li, S. B. Li, W. B. Cao, W. H. Li, W. J. Wen, and G. Alici, *J. Micromech. Microeng.* **22**, 095001 (2012).
- ²⁴Y. C. Lam, H. Y. Gan, N. T. Nguyen, and H. Lie, *Biomicrofluidics* **3**, 014106 (2009).
- ²⁵K. E. Jensen, P. Szabo, F. Okkels, and M. A. Alves, *Biomicrofluidics* **6**, 044112 (2012).
- ²⁶D. L. Lee, H. Brenner, J. R. Youn, and Y. S. Song, *Sci. Rep.* **3**, 3258 (2013).
- ²⁷P. C. Sousa, F. T. Pinho, M. S. N. Oliveira, and M. A. Alves, *Biomicrofluidics* **5**, 014108 (2011).
- ²⁸Y. J. Kang and S. J. Lee, *Biomicrofluidics* **7**, 054122 (2013).
- ²⁹C. J. Pipe and G. H. McKinley, *Mech. Res. Commun.* **36**, 110–120 (2009).
- ³⁰M. S. N. Oliveira, M. A. Alves, and F. T. Pinho, in *Transport and Mixing in Laminar Flows: From Microfluidics to Oceanic Currents*, 1st ed., edited by R. Grigoriev (Wiley-VCH, 2012).
- ³¹C. L. A. Berli, *Electrophoresis* **34**, 622–630 (2013).
- ³²C. Zhao and C. Yang, *Adv. Colloid Interface Sci.* **201–202**, 94–108 (2013).
- ³³S. Das and S. Chakraborty, *Anal. Chim. Acta* **559**, 15–24 (2006).
- ³⁴S. Chakraborty, *Anal. Chim. Acta* **605**, 175–184 (2007).
- ³⁵C. L. A. Berli and M. L. Olivares, *J. Colloid Interface Sci.* **320**, 582–589 (2008).
- ³⁶C. Zhao, E. Zholkovskij, J. H. Masliyah, and C. Yang, *J. Colloid Interface Sci.* **326**, 503–510 (2008).
- ³⁷A. M. Afonso, M. A. Alves, and F. T. Pinho, *J. Non-Newtonian Fluid Mech.* **159**, 50–63 (2009).
- ³⁸S. Dhinakaran, A. M. Afonso, M. A. Alves, and F. T. Pinho, *J. Colloid Interface Sci.* **344**, 513–520 (2010).
- ³⁹C. Zhao and C. Yang, *Biomicrofluidics* **5**, 014110 (2011).
- ⁴⁰W. Choi, S. W. Joo, and G. Lim, *J. Non-Newtonian Fluid Mech.* **187–188**, 1–7 (2012).
- ⁴¹A. M. Afonso, M. A. Alves, and F. T. Pinho, *J. Colloid Interface Sci.* **395**, 277–286 (2013).
- ⁴²E. Lee, Y. F. Huang, and J. P. Hsu, *J. Colloid Interface Sci.* **258**, 283–288 (2003).
- ⁴³J. P. Hsu and L. H. Yeh, *Langmuir* **23**, 8637–8646 (2007).
- ⁴⁴L. H. Yeh and J. P. Hsu, *Microfluid. Nanofluid.* **7**, 383–392 (2009).
- ⁴⁵A. S. Khair, D. E. Postuszny, and L. M. Walker, *Phys. Rev. E* **85**, 016320 (2012).
- ⁴⁶F. M. Chang and H. K. Tsao, *Appl. Phys. Lett.* **90**, 194105 (2007).
- ⁴⁷R. M. Bryce and M. R. Freeman, *Phys. Rev. E* **81**, 036328 (2010).
- ⁴⁸R. M. Bryce and M. R. Freeman, *Lab Chip* **10**, 1436–1441 (2010).
- ⁴⁹X. Lu, S. Patel, M. Zhang, S. W. Joo, S. Qian, A. Ogale, and X. Xuan, *Biomicrofluidics* **8**, 021802 (2014).
- ⁵⁰L. E. Rodd, T. P. Scott, D. V. Boger, J. J. Cooper-White, and G. H. McKinley, *J. Non-Newtonian Fluid Mech.* **129**, 1–22 (2005).
- ⁵¹J. Soulages, M. S. N. Oliveira, P. C. Sousa, M. A. Alves, and G. H. McKinley, *J. Non-Newtonian Fluid Mech.* **163**, 9–24 (2009).
- ⁵²P. C. Sousa, F. T. Pinho, M. S. N. Oliveira, and M. A. Alves, *J. Non-Newtonian Fluid Mech.* **165**, 652–671 (2010).
- ⁵³J. Y. Kim, S. W. Ahn, S. S. Lee, and J. M. Kim, *Lab Chip* **12**, 2807–2814 (2012).
- ⁵⁴J. Nam, H. Lim, D. Kim, H. Jung, and S. Shin, *Lab Chip* **12**, 1347–1354 (2012).
- ⁵⁵K. W. Seo, Y. J. Kang, and S. J. Lee, *Phys. Fluid.* **26**, 063301 (2014).
- ⁵⁶I. Ermolina and H. Morgan, *J. Colloid Interface Sci.* **285**, 419–428 (2005).
- ⁵⁷J. Zhu, S. Sridharan, G. Hu, and X. Xuan, *J. Micromech. Microeng.* **22**, 075011 (2012).
- ⁵⁸S. Sridharan, J. Zhu, G. Hu, and X. Xuan, *Electrophoresis* **32**, 2274–2281 (2011).
- ⁵⁹I. Wong and C. M. Ho, *Microfluid. Nanofluid.* **7**, 291–306 (2009).
- ⁶⁰J. Zhu and X. Xuan, *Electrophoresis* **30**, 2668–2675 (2009).
- ⁶¹A. M. Afonso, F. T. Pinho, and M. A. Alves, *J. Non-Newtonian Fluid Mech.* **179–180**, 55–68 (2012).
- ⁶²A. Kale, X. Lu, S. Patel, and X. Xuan, *J. Micromech. Microeng.* **24**, 075007 (2014).
- ⁶³R. Pethig, *Biomicrofluidics* **4**, 022811 (2010).
- ⁶⁴S. Senapati, A. R. Mahon, J. Gordon, C. Nowak, S. Sengupta, T. H. Q. Powell, J. Feder, D. M. Lodge, and H. C. Chang, *Biomicrofluidics* **3**, 022407 (2009).
- ⁶⁵I. F. Cheng, S. C. Chiang, C. C. Chung, T. M. Yeh, and H. C. Chang, *Biomicrofluidics* **8**, 061102 (2014).

Biomicrofluidics is copyrighted by AIP Publishing LLC (AIP). Reuse of AIP content is subject to the terms at: <http://scitation.aip.org/termsconditions>. For more information, see <http://publishing.aip.org/authors/rights-and-permissions>.